Journal of Engineering Science and Technology
Special Issue on Development of Sustainability Systems - III, 125 - 146

EVALUATING THE AQUACROP MODEL FOR SIMULATING WINTER WHEAT YIELD AND WATER PRODUCTIVITY IN IRAQ

YAQEEN KAMIL[1,*], MUSTAFA AL-MUKHTAR[1], KHALID SHEMAL[2]

[1]College of Civil Engineering, University of Technology-Iraq
[2]Iraqi Ministry of Water Resources, The General Authority for Irrigation and Reclamation Projects.
*Corresponding Author: bce.21.51@grad.uotechnology.edu.iq

Abstract

Estimating crop water consumption is an important tool for decision-making on food and water security, enhancing water use efficiency and achieving optimal water management and sustainability. This research intends to estimate the water requirements of wheat production and the biomass of four regions within the Euphrates River basin in Iraq, namely, Babylon, Anbar, Najaf, and Diwaniyah cities, using the Aqua-Crop model. The model was initially calibrated and validated under current climate conditions using relevant data from 2007-2022. The collected data included climate, soil, crop, and irrigation of the respective areas. In addition, a variety of irrigation scenarios were postulated to investigate the causal relationships between crop yield and water productivity and irrigation amounts. Results proved a superior performance of the Aqua-Crop model in terms of the statistical indicators used. The wheat production was 8.60, 7.54, 6.88, and 8.42 tons per hectare for Babylon, Anbar, Najaf, and Diwaniyah governorates, respectively. Meanwhile, the biomass amounts were 4.198, 6.573, 9.311, and 5.619 for Babylon, Anbar, Najaf, and Diwaniyah cities, respectively. The estimated water requirement for the chosen period was calculated to be 424, 428, 434, and 420 mm for Babylon, Al-Anbar, Najaf, and Al-Diwaniyah, respectively. The rate of evapotranspiration (ET) estimated by Aquacrop during the period was 489, 490, 472, and 410 mm for Babylon, Anbar, Najaf, and Diwaniyah, respectively. This study can serve as an insightful benchmark for the water management of the Euphrates River basin in Iraq to adopt sustainable and cost-effective water management techniques.

Keywords: Aquacrop, Euphrates River, Iraq, Water requirements, Wheat.

1. Introduction

The water crisis has become a global issue due to the combined effects of socioeconomic development and climate change [1]. One sustainable resource is water, but access to it varies over time, space, and the gap between limited water resources and rising demand is widening [2, 3]. Iraq, as one of the MENA region countries, has been identified as the most water-scarce area in the world owing to its semiarid climate.

Water shortages in Iraq have also resulted from the construction of numerous dams on the Euphrates and Tigris Rivers in Turkey, Syria, and Iran, as well as from induced anthropogenic climate change that increased water demand [4, 5]. Nevertheless, Iraq's irrigation water supplies are not effectively managed. The ample water supply, reliant on the Euphrates and Tigris Rivers, and appropriate rainfall levels in the past prevented this from posing any significant issues.

However, nowadays, owing to the policies pursued by the upstream riparian countries, including reduced river discharge in addition to rising salinity, decreased rainfall, and old irrigation systems, the water crisis has emerged as a more serious issue, hindering proper water management [6]. With the supply estimated to be 43 billion cubic meters (BCM) in 2015 and projected to be 17.6 BCM in 2025, and the present demand being between 66.8 and 77 BCM, these issues are expected to get worse in the future [7, 8].

Wheat is the major crop planted in Iraq, where only 39.7% of the wheat cultivation area is rain-fed (mainly in the northern parts, in favour of climate conditions), and the remainder relies on irrigation (mainly in the southern parts) [9, 10]. About 1,675,427 million hectares of wheat are cultivated in Iraq, and 2,195,574 million tons of wheat were produced during the 2016-2017 growing season. In 2018, a 14% decrease in wheat production was estimated compared to the previous year's level and an almost 20% decline in comparison to the mean of the previous five years [11]. Consequently, currently, Iraq imports 3.4-5 million tons annually as a result of production levels not meeting demand [11].

Using crop models to mimic crop growth has become an essential tool in contemporary agriculture. Popular crop models, including Aqua-Crop, WOFOST, and DSSAT, among others, are commonly used for that purpose. Many researchers have tested the applicability of the AquaCrop model by simulating crop growth across different regions of the world. Jalil et al. [12] used the Aqua-Crop model for wheat crop production, water productivity WP, and biomass production in the Kabul River Basin. They hypothesized four different water scarcity scenarios based on the ratio of soil refilling to field capacity.

Their results demonstrated the superior performance of the Aqua-Crop model, with simulated parameters closely matching observed values. Zeleke and Nendel [13] employed the Aqua-Crop model in South-Eastern Australia to estimate wheat canopy cover, dry aboveground biomass, soil water content, and wheat production. They showed that the model was superior at predicting soil water content and grain yield, albeit with a slight underestimation of dry aboveground biomass in the early period and an overestimation of crop canopy cover during the late development stage.

Kheir et al. [14] compared the APSIM-Wheat and Aqua-Crop models in the Egyptian Nile Delta to estimate wheat yield and water productivity. They proposed various treatment scenarios represented by planting dates, irrigation, and fertilization over two successive winter growing seasons to optimize crop production. Their findings confirmed that both models performed well and can be used to identify the best management strategies.

The applicability of the Aqua-Crop model in arid to semiarid areas in Iran was investigated by Khoshsirat et al. [15]. They used the model to simulate the grain yields of winter wheat and barley under different management scenarios, i.e., full irrigation of 100, 90, 80, 70, 60, and 50% of water requirements. They illustrated that the model can be used for predicting and optimizing winter wheat and barley yields in addition to water productivity under different irrigation treatments.

In the investigation performed by Wang et al. [16], winter wheat canopy cover, grain yield, biomass, soil water content, crop evapotranspiration (ETc), and crop weight per square meter were assessed in relation to irrigation scheduling at field capacities of 50%, 60%, and 70% using sprinkler irrigation, drip irrigation, and flood irrigation techniques. Crops were investigated in the North China Plain. They concluded that the Aqua-Crop model was a viable instrument for more precisely simulating the soil water content, canopy cover, grain yield, biomass, ETc, and WP of winter wheat under various irrigation schedules and methodologies compared to current practices.

Zhai et al. [17] assessed the use of saline water irrigation for optimizing winter wheat production using the Aqua-Crop model in the north of China. They revealed that the model satisfactorily performed, though the model overestimated the soil moisture and wheat production and underestimated the soil salinity. Wang et al. [18] analysed different water and nitrogen application scenarios to optimize winter wheat yield in the Yellow River basin using the Aqua-Crop model. Their findings suggested a superior applicability of the model to simulate the growth process of winter wheat under the proposed water-saving and fertilizer-saving scenarios.

Nevertheless, very few studies have addressed the applicability of the AquaCrop model under Iraqi climate conditions. Euphrates River catchments in Iraq are mostly overlaid with wheat agricultural areas. Therefore, it is critical to validate the suitability of Aqua-Crop for optimizing water management to improve crop productivity in that area. As such, this study focused on estimating wheat production and the water requirements for its cultivation in the irrigated lands of the southern Euphrates River catchments in Babylon, Anbar, Najaf, and Diwaniyah. Previous works came out with the fact that the 15 provinces showed variations in WFs attributed to the difference in climate and production values. The novelty of this study is designated as being the first example of using the Aqua-Crop model to quantify wheat production, water requirements, and water productivity in the arid areas of the south of Iraq.

2. Materials and Methods

2.1. The study area

The area selected for this study was the Euphrates River Basin inside the Iraqi territories. The area encompasses four different locations, i.e., Babylon, Al-Anbar, Najaf, and Al-Diwaniyah cities, located along the river basin within the coordinates 30°-35° N and 40°-45° E, as shown in Fig. 1. The average annual rainfall in the investigated area varies by region, with precipitation falling primarily from October to April. Rainfall exhibits a consistent temporal and spatial distribution. It starts in October, peaks in January, and then progressively declines in February and April.

The region's climate is characterized by cold, brief winters and hot, intense summers, with significant daily and annual temperature variations. Depending on the variables influencing its creation, soil composition differs from location to location. The elevation above sea level that defines the research area varies from location to location, ranging between 21 and 60 m amsl [6].

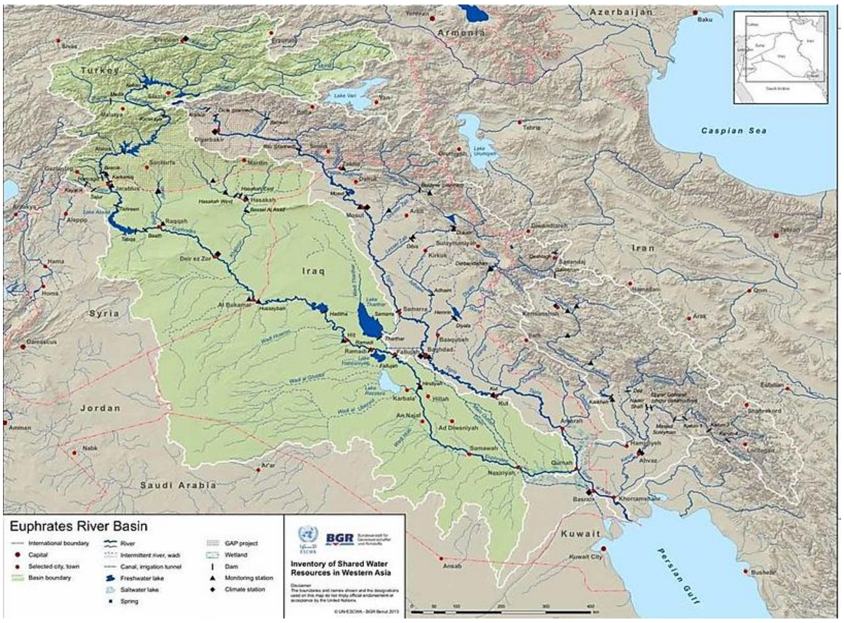

Fig. 1. Location of Euphrates catchment area (source: UN-ESCWA, 2013. PP. 50-51).

2.2. Aqua-Crop model

The model is widely used in agricultural studies due to its accuracy, simplicity, and viability in agricultural water production [19, 20]. The model is a water-driven-based tool that addresses the interaction of soil water alterations on crop growth [21, 22]. It is adopted for a variety of climates and can be considered for future climate scenarios through its functionality of normalizing water productivity (WP) [23].

The Aqua-Crop model created a soil-plant-atmosphere continuum for water interaction in daily steps [24], which is quite useful for continuously monitoring crop development. Besides, some management techniques, e.g., including irrigation, fertilization, and weed control, directly affect crop growth [25]. The primary procedures for grain production and crop development are as follows:

Crop growth: Rather than using leaf area index to characterize crop growth, the Aqua-Crop model uses canopy cover (CC) to compute crop transpiration throughout leaf ageing, senescence, and expansion.

Transport of groups: To determine the transpiration of a crop, multiply the ET_0 by a crop coefficient. The FAO Penman-Monteith equation could determine the ET_0 by utilizing several driven meteorological variables. The crop coefficient adjusted proportionately to CC as the crop canopy developed.

Biomass above ground: Crop transpiration and water productivity are employed to determine the amount of accumulated biomass Eq. (1).

Formation of grain yield: The yield is separately calculated on biomass using the Harvest Index (HI) as given in Eq. 2. The HI increases linearly rather than continuously to the reference Harvest Index (HI_o) from flowering to maturity, which is specific to each cultivar.

$$B = \sum Tr \times WP \tag{1}$$

$$Y = B \times HI \tag{2}$$

where B is biomass, WP is water productivity, Tr is the crop transpiration, HI is harvesting index, and Y is yield. Further model description and analysis can be found in [26].

2.3. Data collection

The Aqua-Crop model demands four kinds of datasets, i.e., meteorological data, crop data, management data, and soil data. The individual description of each set is given below.

2.3.1. Climate data

Meteorological data were obtained from an Automatic Weather Station for each of the respective governorates for the period from 2007 to 2023 based on a daily time scale. The meteorological data were utilized to generate the climate file in Aqua-Crop. The collected data encompasses precipitation, maximum and minimum temperatures, and evaporation. The maximum value of rainfall recorded was less than 50 mm/day for Babylon. On the other hand, temperatures over the evaluated period showed continuous and gradual increases.

In contrast, the reference evapotranspiration, which started at a low level and gradually increased over time, reached its peak during the hot seasons of the year. For Anbar city, the frequency and quantity of rainfall were first low at the beginning of the study period and then gradually increased, reaching their greatest value in 2016, while the temperature reached above 50 °C in 2017. In Najaf, it is evident that the frequency of rainfall in 2015 was high, with a peak value above 35 mm/day.

However, in 2016, the frequency gradually decreased until it reached its lowest recorded value, below 10 mm/day. The precipitation of rain exhibits distinct and precise variations in its quantities, densities, directions, and timings over different spatial and temporal scales, which peaked in 2009 at a value above 70 mm/day. For Diwaniyah, the temperature range with the highest value spans from 55 to 50 °C.

Table 1 lists the Analytical statistics of the collected data for each study site. It presents the main descriptive statistics for three key climatic variables: rainfall, maximum and minimum air temperature, and evapotranspiration across four stations located within the Euphrates River Basin in Iraq, namely, Babylon city, Anbar city, Najaf city, and Diwaniyah city. The statistics displayed include maximum, minimum, mean, standard deviation, and skewness. The table shows substantial spatial variability among the stations. Anbar exhibits the highest maximum rainfall of 80.9 mm, whereas Babylon and Najaf record considerably lower values.

Temperature extremes reflect a highly continental climate, with minimum temperatures reaching as low as -6.5 °C in Anbar city. Evapotranspiration values indicate consistently high evaporative demand across all stations, highlighting the arid and semiarid climatic conditions dominating the Euphrates Basin. The skewness coefficient provides insights into the behaviour of the data distribution. High positive skewness in rainfall and evapotranspiration suggests right-skewed distributions, meaning that most values are low with few high extremes typical for dry and semi-dry environments.

Table 1. Descriptive statistics of rainfall, temperature and evapotranspiration for the selected cities in Iraq.

City	Statistics	Rain (mm)	Temperature (C°)		Evapotranspiration (mm)
			Maximum	minimum	
Babylon	Maximum	39.8	51.7	37	19
	Minimum	0	6.1	-6.2	1.2
	Mean	0.4	30.7	16	5.7
	Standard deviation	2	10.8	9	3.2
	Skewness	8.1	-0.04	-0.03	0.5
Anbar	Maximum	80.9	51.1	36	17
	Minimum	0	4	-6.5	0.7
	Mean	0.3	32	16	5.8
	Standard deviation	2.2	10.7	8.9	3.1
	Skewness	18.7	-0.14	-0.15	0.4
Najaf	Maximum	50.6	48	34	16
	Minimum	0	5	-5	0.3
	Mean	0.2	30.2	15.1	6.1
	Standard deviation	1.5	9.6	8.3	2.9
	Skewness	17	-0.1	-0.04	0.5
Diwaniyah	Maximum	51.6	48	35	16
	Minimum	0	7.29	-6	1.1
	Mean	0.4	32	17	5.4
	Standard deviation	2.3	10.5	8.3	2.8
	Skewness	14	-0.1	-0.2	0.6

2.3.2. Soil data

The Aqua-Crop soil component allows up to five distinct horizons with varying depths and textures. Aqua-Crop necessitates the saturated hydraulic conductivity (Ksat), the volumetric water content at the field capacity (FC), permanent wilting point (PWP), saturation (SAT), and total available water (TAW) for each horizon in the soil profile [27]. Soil samples were collected from two depth ranges between 0.30 m and 0.60 cm, being the effective root depth.

Table 2 presents the primary physical and hydraulic soil properties for the studied sites within the Euphrates Basin. The parameters include soil type, saturated hydraulic conductivity (Ksat), and volumetric soil water content at saturation, field capacity, permanent wilting point, in addition to total available water and the effective root zone depth. The table demonstrates pronounced spatial variability in hydraulic behaviour among the sites.

Loam soils in Babylon exhibit moderate water storage capacity, whereas the silt loam soils of Anbar show notably high hydraulic conductivity, indicating greater permeability. Although Najaf soils share a similar texture with Anbar, they display slightly reduced water retention. In contrast, the sandy loam soils in Diwaniyah show the highest permeability and the lowest water-holding capacity, consistent with sandy-textured soils. These differences underscore the influence of soil texture and hydraulic properties on plant-available water and potential crop responses under current and future climate conditions.

Table 2. Soil properties of the study area.

City	Soil type	Saturated hydraulic conductivity (mm/day)	Soil water content *vol.*%			total available water (mm/m)	Thickness (m)
			SAT	FC	PWP		
Babylon	Loam	350	48	34	15	210	0.3
	Loam	350	48	34	15	191	0.6
Anbar	Silt loam	575	46	33	13	200	0.36
	Silt loam	100	54	50	32	180	0.65
Najaf	Silt loam	400	44	31	13	170	0.3
	Silt loam	400	44	31	13	180	0.6
Diwaniyah	Sandy loam	48.8	50.3	40.7	28.2	200	0.35
	Loam	627.9	55.7	24.5	13.9	180	0.45

2.3.3. Crop data

The crop data required in Aqua-Crop is classified into conservative parameters, nonconservative parameters, and cultivar-specific crops. Tables 3 and 4 describe the wheat temporal data and wheat parameters used in this study, respectively. Five elements of crop data are necessary for Aqua-Crop: phenology, biomass production, rooting depth, canopy cover, and harvestable yield.

Table 3. Temporal crop measurement data in December 2020 of the wheat crop.

Crop parameter	units	Measured data			
		Babylon	Anbar	Najaf	Diwaniyah
Sowing date	d/m/y	5 Dec.	20 Dec.	20 Dec.	24 Dec.
Time to emergence	Day	12	10	14	15
Time to Flowering	Day	98	104	10	90
Maximum canopy cover	Day	100	98	10	101
Maximum root depth	Day	83	139	36	108
Time from sowing to start senescence	Day	111	119	120	109
Time from sowing to start maturity	Day	135	145	145	131

Table 4. Accurate Aqua-crop features for wheat crops.

Agricultural parameter	Value
Conservative constraints	
Initial and Extreme Temperatures (°C)	10, 30
Canopy diminishment factor	6.2%
Canopy development factor	5.5%
Average root zone expansion (cm/day)	0.6
Normalized crop water productivity for climate and CO_2 (tons/hectare)	0.17
Potential percentage rise in harvest index due to water stress earlier than the starting yield development	5%
Reduction of reference water productivity	63%
The shape factor refers to the parameter considered to determine the water stress on canopy expansion	3
***Ksexp,w upper threshold**	0.25
***Ksexp,w lower threshold**	0.55
Shape factor for the water stress coefficient that regulates stomatal regulation	3
$Kssto upper threshold	0.5
Shape factor for the water pressure coefficient that affects canopy aging	3
$Kssen upper threshold	0.85
Potential percentage rise of harvest index (HI) resulting from water stress before the initiation of yield development	10%
The coefficient that positively affects the harvest index by limiting the growth of vegetation during the production of yield	2.7
The coefficient that negatively affects the harvest index by limiting the growth of vegetation during the production of yield	6
Maximum acceptable rise in harvest index	15%
Non-conservative Parameters	
Shape component characterizes the expansion of the root zone	1.5
The minimum depth at which roots can effectively absorb water and nutrients	0.3 m
Average root zone expansion (cm/day)	0.6
The maximum depth at which roots can effectively grow (in meters)	1
The maximum rate at which water is extracted from the soil by the roots, measured in cubic meters of water per cubic meter of soil per day, within the uppermost fourth of the root zone	0.048
The maximum rate at which water is extracted from the soil by the roots, measured in cubic meters of water per cubic meter of soil per day in the lower fourth of the root zone	0.012
The impact of canopy cover on decreasing soil evaporation during the final phase of the growing season	60%
Enhancing the Harvest Index initiates during the root expansion phase, which spans a specific number of days.	252

***Ksexp,w: Canopy expansion water stress coefficient**
$Kssto: Water stress coefficient for canopy senescence

Throughout the growing season, the subsequent phenological stages of the crop were documented: planting date, 90% emergence, commencement of flowering, commencement of senescence, termination of flowering, and maturity. The onset of senescence has been described as that point when the canopy cover commenced to diminish. Table 3 presents the main temporal growth stages of wheat across four Iraqi governorates, highlighting the influence of local environmental and management conditions on crop growth. Sowing dates varied from 5 Dec to 24th, shaping the timing of all subsequent stages. Seedling emergence occurred within 10–15 days, primarily driven by soil temperature and moisture. Flowering showed noticeable spatial variation (90-104 days), reflecting differences in thermal and photoperiodic conditions among the sites.

In contrast, the time required to reach maximum canopy cover was relatively uniform (98-101 days), indicating similar aboveground growth dynamics. Root depth exhibited the greatest variability (36–139), emphasizing the strong effect of soil structure and water availability. Senescence began 109–120 days after sowing, marking differences in the functional length of the growing season. Overall, these temporal parameters provide essential empirical inputs for crop modelling and enhance understanding of wheat responses under diverse agro-ecological conditions.

In aqua-crop, the time to emergence denotes the period of time necessary for ninety percent of the seeds to germinate and endure growth into plants. Aqua-Crop offers crop metrics that exhibit a relatively stable pattern across temporal, spatial, and managerial variations [28]. The conservative parameters under consideration include a range of factors, including coefficients of canopy development and decline, crop coefficients determining transpiration at complete canopy, water productivity from biomass production, concentrations of air CO_2, thresholds for soil water depletion that restrict leaf growth and stomatal conductance, and the acceleration of canopy senescence, as well as the reference harvest index and coefficients utilized to adjust harvest index to correspond with leaf growth and stomata. The information was obtained from the Division of Agricultural Meteorology within the Ministry of Agriculture of Iraq.

A portion of the conservative values was found to be within the range recommended in the Aqua-Crop manual of instructions [23]. The canopy reduction coefficient (CDC) and canopy growth coefficient (CGC) were established at 5.5% and 6.2% per degree day, respectively. Each of the values mentioned falls within the permissible range specified by the CDC (0.004 percent per degree day) and CGC (0.004-0.008 percent per degree day). However, variations were observed in specific supplementary variables, including water productivity (WP) for climate and CO_2. The biomass water productivity value that was assessed during the calibration process for our wheat cultivar was 0.17 tons/ha, which is within the specified range of 0.2 to 0.4.

2.4. Irrigation data

Supplemental irrigation is extremely effective in arid regions with scant or erratic precipitation. There are significant variations among crops due to irrigation. Adjusting the timing of irrigation during crop growth stages, such as panicle initiation and early filling of grains, is necessary for avoiding deficits in water. Supplying plants with the necessary water for their growth for winter wheat crops using surface irrigation (basin irrigation) is extremely productive when integrated with other agricultural activities.

Water scarcity can be mitigated, and sporadic droughts can be better managed through the use of irrigation [29]. Lomling et al. [30] revealed that augmenting irrigation volumes resulted in agricultural yields doubling in comparison to the absence of irrigation. The irrigation started only one day after planting the wheat crop and continued during the growth period with 8 events with a duration between (11-20) days from one time to another. The amount of irrigation ranges between 34-75 mm for Babylon, 30-75 mm for both Anbar and Diwaniyah, and 35-75 mm for Najaf from December or November till the harvesting time.

2.5. Model calibration and validation

The Aqua-Crop model was calculated and validated for two periods. The calibration period spanned from 2007 to 2015, while the validation period included the years 2016 to 2022. The calibration procedure involved iterative adjustments to the crop growth factors, computation of growth coefficients, and other parameters specified in the Aqua-Crop user manual.

The calibrated values were adjusted to minimize the error between the measured and modelled biomass and wheat yields during the two periods. The aqua crop model was subsequently validated using data on aboveground biomass and yield collected from multiple locations within the catchment areas, i.e., Babylon, Anbar, Najaf, and Diwaniyah. More than 50% of the collected data was utilized for calibration, while the remaining portion was allocated for validation.

2.6. The statistical indicators

The coefficient of determination, root mean square error, normalized root mean square error, Nash-Sutcliffe coefficient, and index of agreement were used to assess the model's performance by comparing simulated wheat yield and biomass with observed data. The individual description of each indicator is given below.

2.6.1. Coefficient of determination

The coefficient of determination (R^2) quantifies the proportion of variation accounted for by the model in relation to the observed or measured values. That measures how well the observed values match the simulated values.

$$R^2 = \left[\frac{\sum(o-\overline{o})(p-\overline{p})}{\sqrt{\sum(o-\overline{o})^2(p-\overline{p})^2}}\right] \tag{3}$$

2.6.2. Root means square error

It is one of the most widely used statistical indicators [31]. It measures the average amount of difference between forecasts (Expectations) and observations. The good feature of (RMSE) is that it summarizes the average difference between forecast and observation units.

$$RMSE = \sqrt{\frac{\sum(Pi-Oi)^2}{n}} \tag{4}$$

2.6.3. Normalized root mean square error

It gives an index on the relative difference between model results and observations. The use of NRMSE is more advantageous than root mean square because it enables the comparison of multiple variables [32].

$$\mathrm{NRMSE} = \frac{1}{\bar{O}}\sqrt{\frac{\sum(Pi-Oi)^2}{n}} * 100 \tag{5}$$

2.6.4. Nash- Sutcliffe model efficiency coefficient (EF)

It refers to the extent to which the plot of observed data matches the modelled data. It is frequently utilized to evaluate the effectiveness of hydrological models, as stated by Elsadek et al. [33].

$$EF = 1 - \frac{\sum(Pi-Oi)^2}{\sum(Oi-\bar{O})^2} \tag{6}$$

2.6.5. Willmott's index of agreement

It is employed to assess the accuracy of model predictions by measuring the degree to which the modelled data are close to observed data. It was specifically designed to facilitate interpretation and enable comparisons of model performance [34]. It is calculated by adding the squared absolute values of the distances between the average observed value and the expected value.

$$d = 1 - \frac{\sum(\mathrm{Pi}\text{-}\mathrm{Oi})^2}{\sum(|P-\bar{O}|+|O-\bar{O}|)^2} \tag{7}$$

where P is a simulated value, O is the observed value, $\bar{O}$ is the mean of the observed value, $\bar{P}$ is the mean of the simulated value, and n is the number of observations.

3. Results and Discussion

3.1. Performance of Aqua-Crop

In this study, the Aqua-Crop model was used to assess the deficit in irrigation scenarios on wheat production and biomass for four different agricultural areas along the Euphrates River in Iraq. To this end, the model was calibrated and validated using different datasets from the respective areas. Thence, the real catchment behaviour is represented. The simulation yield was satisfactory across the studied sites.

There was a rather strong correlation between the measured and observed values for both yield and biomass, indicating a reliable simulation of yield and biomass production. Figures 2, 4, 6, and 8 show scatter plots of observed and modelled yield (t/ha) of Babylon, Anbar, Najaf, and Diwaniyah, respectively. Figures 3, 5, 7, and 9 show scatter plots of observed and modelled biomass (t/ha) of Babylon, Anbar, Najaf, and Diwaniyah, respectively. Apparently, the model performed better at reproducing wheat yield and biomass. Ultimately, it is deliverable from the above analysis that the Aqua-Crop model was efficiently performed and hence can be used as an analysis tool to assess the deficit irrigation scenarios on wheat production within the Euphrates River basin in Iraq.

Figure 2 presents a comparison between the simulated yield generated by the model and the field-measured yield across the period of 2007-2022. The two series exhibit a highly consistent pattern, indicating that the model effectively reproduces the actual temporal variation in crop productivity. The plot shows that peaks and declines in the calculated yield closely match those observed in the measured yield, demonstrating the model's ability to capture the influence of climatic and management conditions throughout the growing seasons. Minor differences appear at certain points; however, these deviations remain within acceptable limits for agricultural simulation models and do not indicate any systematic bias.

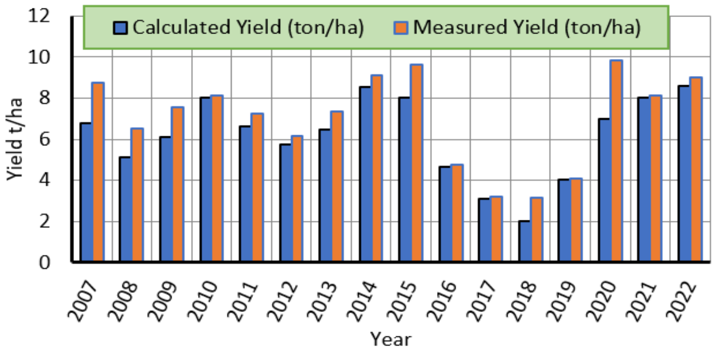

Fig. 2. Calculated and measured yield for the Babylon city.

Figure 3 compares the model-calculated biomass with the measured biomass from field observations. The two datasets exhibit a closely aligned pattern, indicating that the model successfully reflects the actual biomass dynamics over time. A clear correspondence is visible between most simulated and observed values, demonstrating the model's sensitivity to environmental variations that influenced crop growth during the season.

Peaks and troughs appear in nearly the same positions for both series, confirming the model's effectiveness in reproducing the physiological processes contributing to dry matter accumulation. The discrepancies observed at a few points are normal within the context of crop modelling and may result from field variability, measurement uncertainty, or micro-environmental factors.

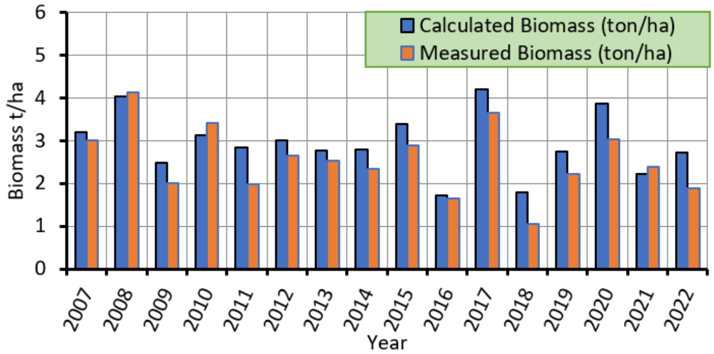

Fig. 3. Calculated and measured biomass for the city of Babylon.

Figure 4 compares the calculated and measured yields for the Anbar site. The results show that the measured yield consistently exceeds the calculated yield, although both series exhibit a similar fluctuation pattern. The parallel trend in both datasets indicates that the applied model can capture the general temporal variability. However, a nearly constant gap between the two curves suggests the need to refine the model parameters or incorporate additional variables to enhance their predictive accuracy.

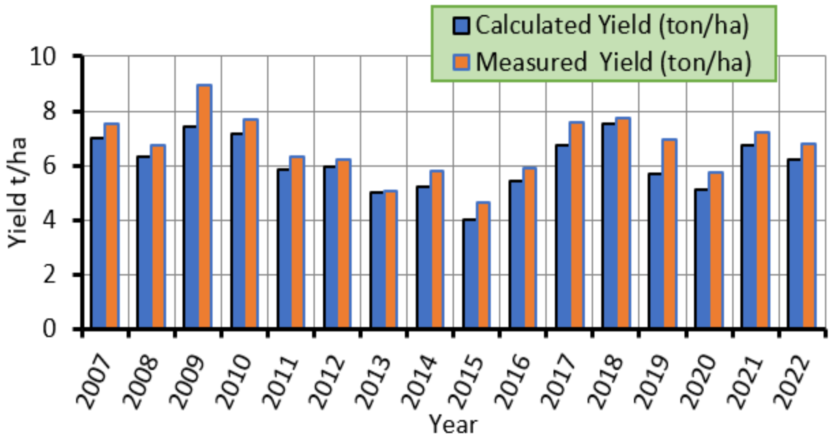

Fig. 4. Calculated and measured yield for Anbar city.

Figure 5 presents a direct comparison of the calculated and measured biomass for Anbar city. The general pattern of variation in the calculated values closely matches the trend observed in the field measurements, indicating a reasonable level of agreement between the model outputs and the actual observations. Although slight discrepancies appear at several points, particularly where sharp increases occur, the overall deviation remains minimal.

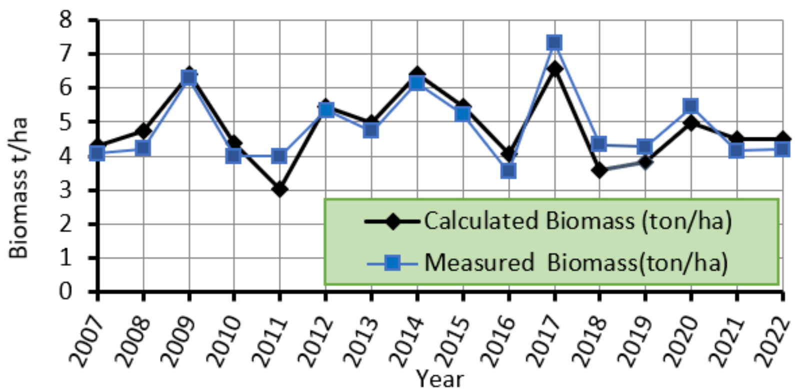

Fig. 5. Calculated and measured biomass for Anbar city.

Figure 6 compares the calculated yield and the measured yield for the Najaf site. The two curves exhibit a similar temporal pattern, indicating that the model effectively captures the overall trend of yield variation. Measured yield values range approximately from 6 to 9 t/ha, while calculated values fall between 5 and 8 t/ha. Noticeable deviations appear at points 7, 10, and 15, where the relative error is higher compared to other points. Despite these differences, the overall agreement between the two datasets remains strong. A positive correlation is evident between calculated and measured yields due to their similar fluctuation pattern.

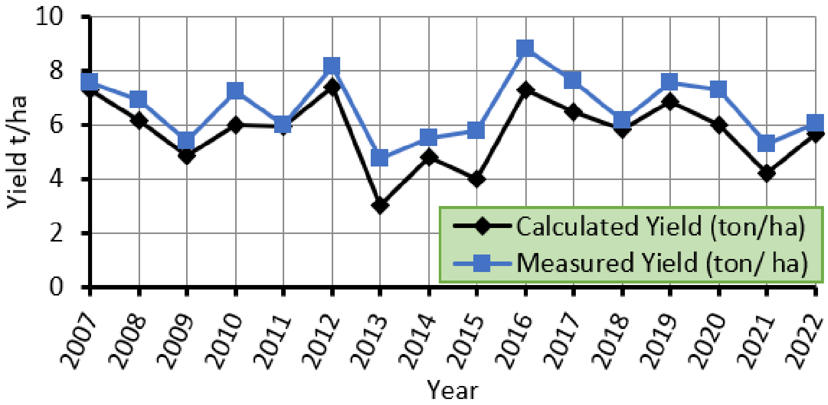

Fig. 6. Calculated and measured yield for Najaf city.

Figure 7 compares the calculated and measured biomass at the Najaf site. The two curves demonstrate a clear similarity in their overall trend, indicating a strong positive correlation between the datasets. Measured biomass values range approximately from 5 to 11, while calculated biomass ranges between 4 and 10. Although slight deviations occur at certain points, the two curves exhibit a high degree of correlation due to their similar fluctuation patterns.

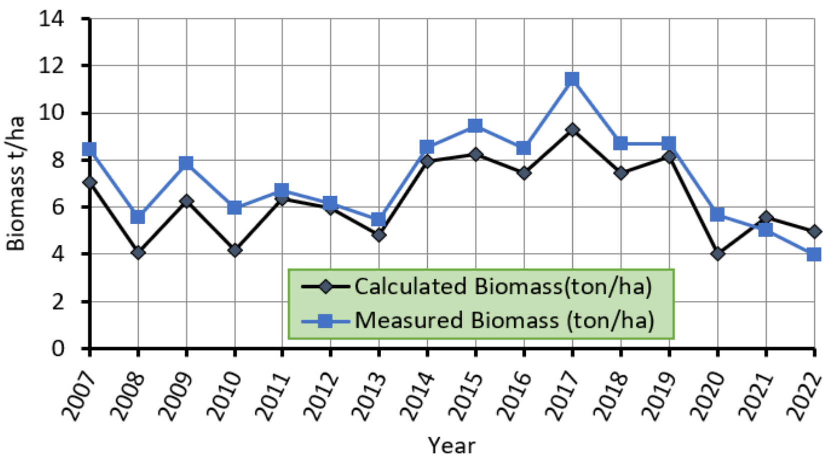

Fig. 7. Calculated vs measured biomass for Najaf city.

Figure 8 illustrates a comparison between the calculated yield generated by the AquaCrop model and the measured field yield of wheat at Diwaniyah city. It can be seen that both curves exhibit a similar temporal pattern, indicating that the model effectively captures the actual seasonal variations in yield.

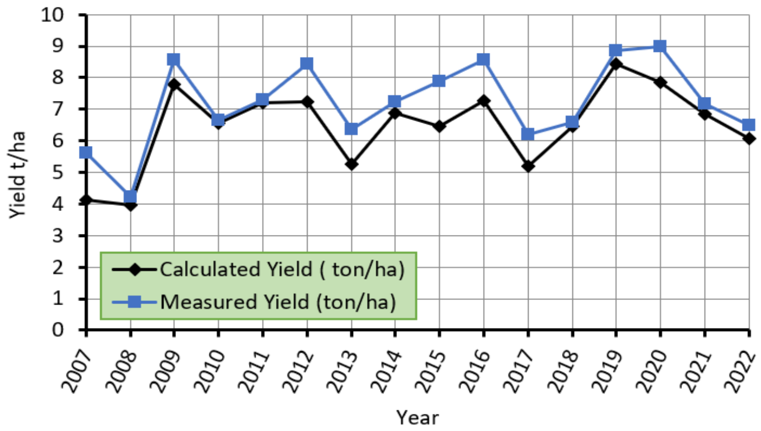

Fig. 8. Calculated and measured yield for Diwaniyah city.

In several points, the model output shows a very strong agreement with the measured yield, demonstrating high model accuracy. However, minor deviations were reported in some points. These discrepancies remain within acceptable limits. The simultaneous behaviour of both curves shows that AquaCrop accurately models the effects of climate, water use, crop phenology, and scientific implications. Lastly, the calculated versus measured biomass at Diwaniyah was depicted as shown in Fig. 9. Several points demonstrate a close match between simulated and measured values, reflecting a satisfactory level of agreement between model performance and field observations. Minor discrepancies appear at certain stages, which is expected in crop modelling due to the sensitivity of biomass to subtle field variations.

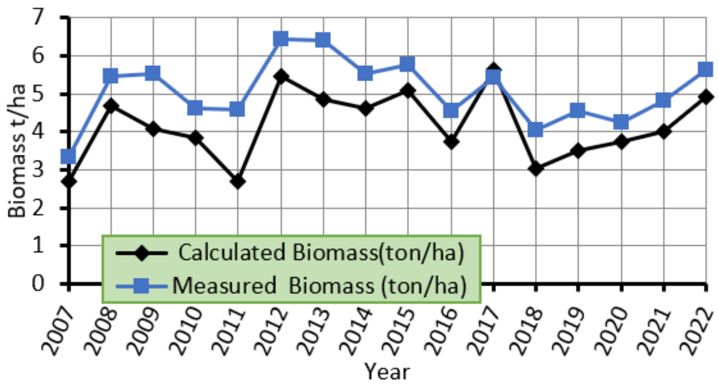

Fig. 9. Calculated and measured biomass for Diwaniyah city.

3.2. Variability of the wheat yield and Biomass

To investigate the spatial and temporal variability in wheat yield and biomass across the four sites in the Euphrates catchment, the calibrated model was applied under current climate conditions from 2007 to 2022. The Aquacrop model estimated the current period's wheat yield and biomass results. From 2007 to 2022, the highest/lowest yield was recorded in 2022/2018 in Babylon, at 8.6/2 ton/ha.

The highest/ lowest yield was recorded during 2018/2015 in Anbar, which was 7.5/4.1 tons/ha. The highest/ lowest yield of Najaf was during 2012/2013, at 7.3/3.1. Lastly, the highest/lowest yield of Diwaniyah was in 2019/2008, with 8.4/3.9 ton/ha. In the same manner, the highest/ lowest biomass was recorded during 2017/2016 in Babylon, with an amount of 4.1/1.8 ton/ha. The highest/ lowest biomass was recorded during 2017/2011 in Anbar, at 6.5/3.1 tons/ha. The highest/ lowest biomass of Najaf was during 2017/2020, with an amount of 9.3/4 ton/ha. Lastly, the highest/ lowest biomass of Diwaniyah was during 2017/2011, at 5.6/2.7 tons/ha.

3.3. Evaluation of water scenarios and wheat productivity

Using the AquaCrop model, the crop water requirements (WR) of wheat in the Euphrates River basin were simulated during the period from 2007 to 2022. The highest/lowest water requirements were recorded in 2022/2018 in Babylon, at 0.43/0.42 m. The highest/lowest water requirements were recorded in 2018/2013 in Anbar, at 0.5/0.48 m. The highest/ lowest water requirement for Najaf was in 2018/2013, at 0.44/0.41 m. Lastly, the highest/lowest water requirements in Diwaniyah were in 2018/2013, at 0.42/0.4 m.

In the same manner, the highest/lowest evapotranspiration water productivity (WPet) for Babylon estimated by Aqua-Crop was during 2022/2007 with an amount of 1.4/0.63 kg/m^3. The highest/lowest evapotranspiration water productivity for Anbar was during 2010/2020, at 1.08/0.79 kg/m^3. The highest/lowest evapotranspiration water productivity for Najaf was during 2022/2018, with an amount of 1.62/0.7 kg/m^3. Lastly, the highest/lowest evapotranspiration water productivity for Diwaniyah was during 2021/2011, with an amount of 1.58/0.9 kg/m^3.

3.4. Effects of irrigation deficit on wheat productivity

Irrigations are occasionally administered at frequent intervals, considering the specific water requirements of the crops. Reducing the amount of water available or increasing the amount available leads to a decrease in water productivity, measured as the yield per unit of water used. In this case, several scenarios were hypothesized and configured by reducing the irrigation water depth by 25%, 50%, and 75% of the full water depth for each area to investigate biomass and yield responses to irrigation water depth deficits.

Insufficient water availability during the process of grain filling results in the production of grain that is shrivelled and has a low milling percentage, which refers to the amount of flour produced per unit of grain input. Tables 5 and 6 illustrate the percentage change in yield and biomass with respect to irrigation deficit, respectively.

When the irrigation water depth was reduced by 25% (the first scenario), yield production for the winter wheat crop declined by 7 to 8% for Babylon, with the highest/lowest value during 2014/2019 of 7.9/4 ton/ha. While for Anbar the percentage of decline was from 15% (6.84 ton/ha) to 16 % (4.19 ton /ha), which aligns with the highest /lowest value during 2018/2013. The percentage decline in Najaf was 12% (4.3 ton/ha) to 15% (8.2 ton/ha), corresponding to the lowest/highest values during 2021/2016.

For Diwaniyah, the percentage of change was 9% to 13%, with the highest /lowest value during 2020/2017 being 7.3/4.7 ton/ha. Similarly, in the second scenario, when the irrigation water depth was reduced to half, yield production decreased by 12% (2.6 ton/ha) to 16% (7.5 ton/ha) in Babylon, representing the highest/lowest value observed during 2022/2017.

For Anbar, the percentage change was 30% (3.6 ton/ha) to 33% (7 ton/ha), in agreement with the highest/lowest values, which occurred in 2022 and 2012/2012. For Najaf, the percentage decline was 30% (3 ton/ha) to 34% (7.2 ton/ha), corresponding to the highest/lowest, which were in 2021/2016, respectively. For Diwaniyah, the percentage of change was from 12% (3.6 ton/ha) to 17% (6.9 ton/ha), matching the highest/lowest value during 2009/2007.

In the third scenario, where the irrigation water depth declined by 75%, yield production in Babylon was reduced by 20% (1.7 ton/ha) to 40% (6.3 ton/ha), which coincides with the highest/lowest value observed during 2014/2018. For Anbar, the percentage of change was from 38% (2.8 ton/ha) to 40% (5.4 ton/ha), which corresponds to the highest /lowest value during 2022/2013. For Najaf, the percentage of reduction was from 50 (4.7 ton/ha) to 65% (2.1 ton/ha), corresponding to the highest /lowest value, which was during 2012/2018. For Diwaniyah city, the percentage of decline was from 28% (2.7 ton/ha) to 47% (5.73 ton/ha), which corresponds to the highest /lowest value during 2019/2007.

Biomass production was also influenced by the irrigation-deficit scenarios. Under the first scenario, i.e. declined irrigated water depth by 25 %, the highest /lowest value of Babylon during 2016/2018 was 6.5/1.5 tons /ha, representing a percentage of change from 11 % to 15%. The highest /lowest values of Anbar were during 2012/2016, which were 6.9/3.6 tons/ha, representing a 10% to 14% decline. The highest /lowest values of Najaf were during 2018/2010, which were 7.8/4.1 ton/ha, referring to a percentage reduction of 4/13%. For Diwaniyah, the highest /lowest biomass was during 2012/2019, which was 5.2/3.4 tons/ha, with the percentage of reduction ranging between 7 to 9%.

Table 5. Percentage of change in yield under declining irrigated water depth.

Percentage of decline in water depth	Percentage of change for each site			
	Babylon	Anbar	Najaf	Diwaniyah
25%	7-8%	15-16%	12-15%	9-13%
50%	12-16%	30-33%	30-34%	12-17%
75%	20-40%	38-40%	50-65%	28- 47%

Table 6. Percentage of change for biomass under declining irrigated water depth.

Percentage of decline in water depth	Percentage of change for each site			
	Babylon	Anbar	Najaf	Diwaniyah
25%	11-15%	10-14%	4-13%	7-9%
50%	10-20%	17-26%	20-25%	16-19%
75%	22-40%	20-43%	25-49%	23-37%

The analysis of the second scenario, a 50% reduction in irrigation, revealed that the highest/lowest biomass in Babylon city occurred during 2015/2018, at 6/1.4 tons/ha, representing a 10/20% decline. Similarly, the highest/lowest biomass of

Anbar were during 2009/2016, which were 6/3.1 tons/ha, approximately a 17% to 27% of reduction. The highest/lowest biomass of Najaf were during 2017/2010, which were 7.3/3.1 ton/ha, which corresponds to a 20/25% of reduction. The highest/lowest biomass of Diwaniyah city was during 2017/2018, which was 4.8/2.8 ton/ha with a percentage of reduction ranging between 16/19%.

In the same manner, the analysis of the third scenario (75% deficit in irrigation) demonstrated that the highest/lowest biomass in Babylon city occurred in 2015/2008, at 4.2/1.1 ton/ha, with a percentage change of 22%/40%. While for Anbar, the highest /lowest biomass were during 2015/2021, which were 5.7/3.1 ton/ha, corresponding to 20% to 43% of reduction. For Najaf, the highest /lowest biomass were during 2014/2020, which was 5.8/1.6 tons/ha, referring to 25%/49% of reduction. Lastly, the highest /lowest biomass of Diwaniyah were during 2014/2007, which were 4.2/2.1 tons/ha, which represents a 23%/37% of reduction.

The evaluation of the AquaCrop model in this study aimed to optimize irrigation management for wheat prediction across four agricultural areas along the Euphrates River in Iraq. As presented above, the model performance was found to be superior in terms of the statistical indices used. Other studies have reported the model's performance capabilities for various crops [18, 35]. For example, Khorsand et al. [35] used the AquaCrop model under climate conditions of semiarid areas in Iran to simulate canola growth. They reported that, based on the model evaluation, the biomass and yield were accurately predicted.

Li et al. [36] calibrated the AquaCrop model utilizing data from forty locations in three of China's most important cotton-growing regions. It was disclosed that the model demonstrated satisfactory functionality in simulating the cotton growth process within the designated study areas. In another study by Bian et al. [37], an accurate simulation of the canopy cover, biomass, WP, and cotton yield of saline - alkali soil was indicated in a study area in Western China using the AquaCrop model.

The AquaCrop model shows an overestimation of wheat yield throughout most of the period and an underestimation in 2010 for the Babylon site. The model shows an overestimation of wheat biomass for the Najaf and Diwaniyah sites during the whole period and an underestimation for the Babylon and Anbar sites during the period 2007-2014. The highest wheat biomass was recorded at the Najaf site, and the lowest was at the Babylon site. The highest wheat water requirement and evapotranspiration water productivity were found in the Anbar and Najaf sites, respectively. The lowest ones were at the Diwaniyah and Babylon sites, respectively. The above variations could be attributed to the influence of climate dynamicity on crop development, which results in diverse growing conditions.

The highest crop yield was recorded in Babylon, and the lowest was recorded in Diwaniyah. This might be due to the climate characteristics and soil fertility conditions of the Babylon site compared to the Diwaniyah site. The comparison of calculated and observed yield ratios demonstrates substantial yield losses caused by water stress. As such, improved time management for irrigation practices must be recommended to increase wheat yield [38]. The presented AquaCrop results seem firmly established for subsequent wheat simulation research. An alternative explanation for the discrepancy between the yield achieved and the yield observed might be variations in drainage conditions in the field [39, 40]. The AquaCrop model simulates drainage when moisture levels exceed the soil field capacity and is unable to account for preferential flows in field conditions.

Additionally, numerous producers assert that entire crop failure seasons have been caused by brief periods of excessive soil moisture. Despite these limitations, the model achieved moderate accuracy in simulating the biomass and yield of the cultivar applied at the sites. Araya et al. [41] reported that adjusting the planting date of a crop can increase crop productivity and biomass. Additionally, early sowing has the potential to mitigate water stress that may arise during the cereal filling phase [42]. It can be concluded that the wheat crop under investigation at this research site exhibited a critical reaction when subjected to water-stressful circumstances (deficit irrigation), which can reduce crop productivity.

4. Conclusion

This study evaluates the performance of the AquaCrop model for predicting the wheat yield and biomass variations in the Euphrates River basin in Iraq. The model was further used to assess the impacts of deficit irrigation scenarios on the wheat characteristics. It was concluded that the AquaCrop model accurately predicts the biomass and yield of winter wheat in the Euphrates catchment area. Enhancing crop productivity and biomass is increasingly significant in regions susceptible to climate change. The degree of fit of the statistics suggested that the model was adequately calibrated and validated for the given biomass and yield parameters of the winter wheat crop.

The results mentioned previously demonstrate Aqua-Crop's accuracy in simulating crop yields and biomass, even for underutilized and neglected crops. AquaCrop has shown its durability as well as accuracy as a crop-water productivity model, which only takes a small amount of easily understood and readily available data. In addition, given that the model can be used to accurately and reliably identify the minimum sensitivity stages and stress thresholds throughout the crop growth period when subjected to moderate water stress, this tool proves to be valuable in the development and assessment of low-irrigation strategies.

Acknowledgments

The authors are grateful for the generous funding and support received from the General Authority for Irrigation and Reclamation Projects during the period of this study.

References

1. Upreti, D.; Pignatti, S.; Pascucci, S.; Tolomio, M.; Huang, W.; and Casa, R. (2020). Bayesian calibration of the Aquacrop-OS model for durum wheat by assimilation of canopy cover retrieved from VENµS satellite data. *Remote Sensing*, 12(16), 2666.
2. Elliott, J. et al. (2014). Constraints and potentials of future irrigation water availability on agricultural production under climate change. *Proceedings of the National Academy of Sciences*, 111(9), 3239-3244.
3. Takács, S.; Csengeri, E.; Pék, Z.; Bíró, T.; Szuvandzsiev, P.; Palotás, G.; and Helyes, L. (2021). Performance evaluation of Aquacrop model in processing tomato biomass, fruit yield and water stress indicator modelling. *Water*, 13(24), 3587.

4. Al-Ansari, N.; Abdellatif, M.; Ezeelden, M.; Ali, S.S.; and Knutsson, S. (2014). Climate change and future long term trends of rainfall at north-eastern part of Iraq. *Journal of Civil Engineering and Architecture*, 8(6), 790-805.
5. Abdulrahman, S.A. (2020). Water shortage in GCC countries: Transferring water from Iraqi Kurdistan Region. *International Journal of Environmental Studies*, 77(2), 191-207.
6. Ewaid, S.H.; Abed, S.A.; and Al-Ansari, N. (2019). Water footprint of wheat in Iraq. *Water*, 11(3), 535.
7. Al-Ansari, N.; Adamo, N.; Sissakian, V.K.; Knutsson, S.; and Laue, J. (2018). Water resources of the Euphrates River catchment. *Journal of Earth Sciences and Geotechnical Engineering*, 8(3), 1-20.
8. Todd, E.C.D. (2024). Waterborne diseases and wastewater treatment in Iraq. *Journal of Food Protection*, 87(1), 100204.
9. USDA Foreign Agricultural Service (2017). Iraqi wheat production down; weather, procurement drop, and conflict to blame. Retrieved October 5, 2025, from https://apps.fas.usda.gov/newgainapi/api/report/downloadreportbyfilename?filename=Grain%20and%20Feed%20Annual_Baghdad_Iraq_10-10-2017.pdf.
10. Terán-Chaves, C.A.; García-Prats, A.; and Polo-Murcia, S.M. (2022). Calibration and validation of the FAO aquaCrop water productivity model for perennial ryegrass (Lolium perenne L.). *Water*, 14(23), 3933.
11. Jassim, H.I. (2018). *Wheat Production in Iraq for the Agricultural Season* (2016–2017). Iraqi Ministry of Agriculture, Office of the Inspector-General, Baghdad, Iraq.
12. Jalil, A.; Akhtar, F.; and Awan, U.K. (2020). Evaluation of the AquaCrop model for winter wheat under different irrigation optimization strategies at the downstream Kabul River Basin of Afghanistan. *Agricultural Water Management*, 240, 106321.
13. Zeleke, K.; and Nendel, C. (2020). Testing and application of the AquaCrop model for wheat production under different field management conditions in South-Eastern Australia. *Agricultural Research*, 9(3), 379-391.
14. Kheir, A.M.S.; Alkharabsheh, H.M.; Seleiman, M.F.; Al-Saif, A.M.; Ammar, K.A.; Attia, A.; Zoghdan, M.G.; Shabana, M.M.A.; Aboelsoud, H.; and Schillaci, C. (2021). Calibration and validation of AQUACROP and APSIM models to optimize wheat yield and water saving in arid regions. *Land*, 10(12), 1375.
15. Khoshsirat, A.M.; Najarchi, M.; Jafarinia, R.; and Mokhtari, S. (2022). Sensitivity analysis and determination of the optimal level of water use efficiency for winter wheat and barley under different irrigation scenarios using the AquaCrop model in arid and semiarid climatic conditions (case study: Dehloran Plain, Iran). *Water*, 14(21), 3455.
16. Wang, G.; Mehmood, F.; Zain, M.; Hamani, A.K.M.; Xue, J.; Gao, Y.; and Duan, A. (2022). AquaCrop model evaluation for winter wheat under different irrigation management strategies: A case study on the North China Plain. *Agronomy*, 12(12), 3184.
17. Zhai, Y.; Huang, M.; Zhu, C.; Xu, H.; and Zhang, Z. (2022). Evaluation and application of the AquaCrop model in simulating soil salinity and winter wheat yield under saline water irrigation. *Agronom*y, 12(10), 2313.

18. Wang, S.; Wang, D.; Liu, T.; Liu, Y.; Luo, M.; Li, Y.; Zhou, W.; Yang, M.; Liang, S.; and Li, K. (2024). Simulation of winter wheat growth dynamics and optimization of water and nitrogen application systems based on the Aquacrop model. *Agronomy*, 14(1), 110.
19. Vanuytrecht, E.; Raes, D.; Steduto, P.; Hsiao, T.C.; Fereres, E.; Heng, L.K.; Vila, M.G.; and Moreno, P.M. (2014). AquaCrop: FAO's crop water productivity and yield response model. *Environmental Modelling & Software*, 62, 351-360.
20. Hamdi, L.; and Suleiman, A. (2024). Evaluating the performance of the AquaCrop model to soil salinity in Jordan Valley. *Jordan Journal of Agricultural Sciences*, 20(2), 87-95.
21. Ahmadi, M.; Etedali, H.R.; Salem, A.; Al-Mukhtar, M.; and Elbeltagi, A. (2024). Simulation of wheat water footprint using Aquacrop model under the climate change, case study in Qazvin plain. *Applied Water Science*, 14(12), 264.
22. Amirouche, M.; Smadhi, D.; and Zella, L. (2021). Calibration and validation of the AquaCrop model for the culture lettuce (Lactuca sativa L.) under fertilization levels in pluvial conditions. *Agricultural Engineering International*: *CIGR Journal*, 23(1), 36-46.
23. Mansour, H.A.; Khalil, S.E.; and Attia, S.S. (2025). Aquacrop Model Validation and Calibration for Full and Deficit Irrigation for Sugar Beets. *Egyptian Journal of Botany*, 65, 23-33.
24. Araya, A.; Keesstra, S.D.; and Stroosnijder, L. (2010). Simulating yield response to water of Teff (Eragrostis tef) with FAO's AquaCrop model. *Field Crops Research*, 116(1-2), 196-204.
25. Zhang, C.; Xie, Z.; Wang, Q.; Tang, M.; Feng, S.; and Cai, H. (2022). AquaCrop modeling to explore optimal irrigation of winter wheat for improving grain yield and water productivity. *Agricultural Water Management*, 266, 107580.
26. Zhai, Y.; Huang, M.; Zhu, C.; Xu, H.; and Zhang, Z. (2022). Evaluation and application of the AquaCrop model in simulating soil salinity and winter wheat yield under saline water irrigation. *Agronomy*, 12(10), 2313.
27. Guo, D.; Olesen, J.E.; Pullens, J.W.M.; Guo, C.; and Ma, X. (2021). Calibrating AquaCrop model using genetic algorithm with multi - objective functions applying different weight factors. *Agronomy Journal*, 113(2), 1420-1438.
28. Nasrolahi, A.H.; Ahmadee, M.; and Rustum, R. (2024). Sensitivity analysis of AquaCrop model for winter wheat in different water supply conditions. *Journal of Irrigation and Drainage Engineering*, 150(2), 04024002.
29. Amiri, E.; Bahrani, A.; Irmak, S.; and Mohammadiyan Roshan, N. (2022). Evaluation of irrigation scheduling and yield response for wheat cultivars using the AquaCrop model in an arid climate. *Water Supply*, 22(1), 602-614.
30. Lomeling, D.; Kenyi, M.M.; Abass, A.A.; Otwari, S.M.; and Khater, Y.M. (2014). Using the CROPGRO model to predict phenology of cowpea under rain-fed conditions. *International Journal of Plant & Soil Science*, 3(7), 824-844.
31. Abdou, S.M.M.; Engel, B.A.; Emam, S.M.; and El-Latif, K.M.A. (2022). AquaCrop model validation for simulation wheat productivity under water stress condition. *Communications in Soil Science and Plant Analysis*, 53(3), 281-292.

32. Yang, J.M.; Yang, J.Y.; Liu, S.; and Hoogenboom, G. (2014). An evaluation of the statistical methods for testing the performance of crop models with observed data. *Agricultural Systems*, 127, 81-89.
33. Elsadek, E.; Zhang, K.; Mousa, A.; Ezaz, G.T.; Tola, T.L.; Shaghaleh, H.; Hamad, A.A.A.; and Alhaj Hamoud, Y. (2023). Study on the in-field water balance of direct-seeded rice with various irrigation regimes under arid climatic conditions in Egypt using the AquaCrop model. *Agronomy*, 13(2), 609.
34. Mabhaudhi, T.; Modi, A.T.; and Beletse, Y.G. (2014). Parameterisation and evaluation of the FAO-AquaCrop model for a South African taro (Colocasia esculenta L. Schott) landrace. *Agricultural and Forest Meteorology*, 192-193, 132-139.
35. Khorsand, A.; Dehghanisanij, H.; Heris, A.M.; Asgarzadeh, H.; and Rezaverdinejad, V. (2024). Calibration and evaluation of the FAO AquaCrop model for canola (Brassica napus) under full and deficit irrigation in a semiarid region. *Applied Water Science*, 14(3), 56.
36. Li, N.; Li, Y.; Yang, Q.; Biswas, A.; and Dong, H. (2024). Simulating climate change impacts on cotton using the AquaCrop model in China. *Agricultural Systems*, 216, 103897.
37. Bian, M.; Lv, T.; Li, W.; Chen, C.; Zhang, X.; and Wang, M. (2025). Effect of irrigation amount on cotton growth and optimization of irrigation regime using AquaCrop in Southern Xinjiang. *Agronomy*, 15(5), 1101.
38. Tang, P.; Li, N.; Li, M.; Zhang, F.; Fu, Q.; Xu, Y.; and Liu, D. (2023). Rice irrigation water efficiency improvement: An AquaCrop-based optimization modeling approach. *European Journal of Agronomy*, 148, 126867.
39. Corbari, C.; Charfi, I.B.; and Mancini, M. (2021). Optimizing irrigation water use efficiency for tomato and maize fields across Italy combining remote sensing data and the Aquacrop model. *Hydrology*, 8(1), 39.
40. Zhang, T.; Zuo, Q.; Ma, N.; Shi, J.; Fan, Y.; Wu, X.; Wang, L.; Xue, X.; and Ben-Gal, A. (2023). Optimizing relative root-zone water depletion thresholds to maximize yield and water productivity of winter wheat using AquaCrop. *Agricultural Water Management*, 286, 108391.
41. Araya, A.; Habtu, S.; Hadgu, K.M.; Kebede, A.; and Dejene, T. (2010). Test of the AquaCrop model in simulating biomass and yield of water deficient and irrigated barley (Hordeum vulgare). *Agricultural Water Management*, 97(11), 1838-1846.
42. Boulange, J.; Nizamov, S.; Nurbekov, A.; Ziyatov, M.; Kamilov, B.; Nizamov, S.; Abduvasikov, A.; Khamdamova, G.; and Watanabe, H. (2025). Calibration and validation of the AquaCrop model for simulating cotton growth under a semiarid climate in Uzbekistan. *Agricultural Water Management*, 310, 109360.